Near-surface salt dissolution void identification using passive MASW

Jeffery J. Nolan, Richard Miller, Julian Ivanov, Shelby Peterie, Kansas Geological Survey; Ed Lindgren, Burns & McDonnel*

Summary

Near-surface voids occur in a variety of settings and from a variety of different sources ranging from natural dissolution features to man-made illegal cross-border tunnels. The detection of these typically air-filled voids using geophysical techniques is surprisingly difficult for an array of factors, despite the drastic change in mechanical properties of the rock. However, it is vital to efficiently and accurately image these voids and surrounding rock properties due to the potential implications for the environment and culture. Passive seismic surveys above known salt dissolution voids were conducted to calculate overlying rock properties and evaluate potential for imminent collapse. Passive multichannel analysis of surface waves (MASW) recorded the necessary low frequencies to image anomalous velocity zones as deep as 90 meters below ground surface. Results of this experiment correlate well with all data at this site, identifying zones of increased shear wave velocity above voids remaining from solution mining of salt in the early 1900's.

Introduction

Void locating using geophysical methods, in theory, should be a relatively easy target due to the drastic changes in properties from the surrounding rock to the air or water filled void. However, in practice, without a priori information successful identification of subsurface voids has been exceedingly challenging. Many geophysical methods have attempted detect voids including gravity (Butler, 1984), ground penetrating radar (Fenner, 1995), and electromagnetic (Keiswetter and Won, 1997). However, of each of these methods, seismic has typically been the most successful (Miller & Steeples, 1991; Nolan et al., 2011; Sloan et al., 2010; Turpening, 1976).

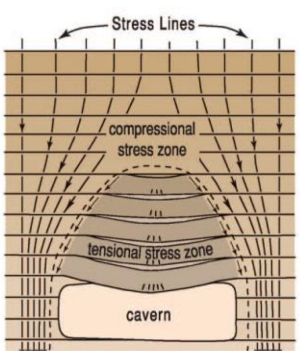

Figure 1. Cartoon representing the increased stress above a subsurface void.

Void detection in the near surface using seismic methods has been utilized to including reflection, refraction, body wave diffraction, surface wave analysis, and surface wave backscatter (Sloan et. al, 2010; Nolan et. al, 2011; Walters et. al, 2009; Landa et. al, 1987). Reflection and refraction surveys typically deal with a depth range of 10's to 100's of meters into the subsurface with frequencies above 50 Hz. The multichannel analysis of surface waves (MASW) method deals with frequencies much lower (~1-30 Hz) and images significantly shallower than the reflection and refraction techniques (Miller et. al, 1999).

Surface wave analysis in the near surface is rapidly increasing in environmental, geotechnical, and engineering applications. The MASW method inverts Rayleigh wave energy into shear wave velocities (Vs), directly relating to the physical properties of the rock. Void identification is possible using MASW due to the increase in shear stress above the void or cavern, therefore increasing shear wave velocity in this tensional stress zone as seen in Figure 1 (modified from Davies, 1951). In a velocity profile, a mature void would have dome shaped increase in velocity above the void.

The MASW method focuses on the dispersion of Rayleigh-type surface waves (Park et al., 1999). Each frequency of a surface wave travels at a different velocity, a property known as dispersion. Higher frequencies sample shallower depths due to lower velocities, while lower frequencies sample the deeper regions. Lateral changes in Vs are imaged using MASW because a large portion of the Rayleigh wave is shear.

The typical active MASW seismic survey uses a controlled source, such as an accelerated weight drop or a sledgehammer. These sources have traditionally been depth limited due to the minimal production of low frequencies. An alternative approach for characterizing deeper depths than possible with active sources is to use a passive survey approach, to obtain a velocity profile. The passive surface wave method is an alternative to the active survey method, which often does not achieve sufficient depth of investigation (Park and Miller, 2008).

The use of ambient noise, whether that is cultural or natural, can be used to obtain some of the lower frequencies that active surveys lack. Orienting the survey line to optimally acquire the minimum apparent phase

DOI http://dx.doi.org/10.1190/segam2013-1146.1

velocity of surface waves from nearby trains proved effective in recording ample low frequency signal for our survey depths of 90 meters.

Geologic Setting

The test site is located in south-central Kansas near the city of Hutchinson. Figure 2 shows the generalized geology of the common seismic reflectors in the test area. Approximately 65 meters of coarse alluvial unconsolidated sands and gravel lie at the surface, underlain by the Pleistocene beds known as the Equus beds. Another strong seismic reflector is the Permian Ninnescah Shale. The Permian Wellington Formation is separated in many places by this Hutchinson Salt Member. The upper and lower portions consist of shales while the middle is anhydrites and shale stringers interbedded in salt.

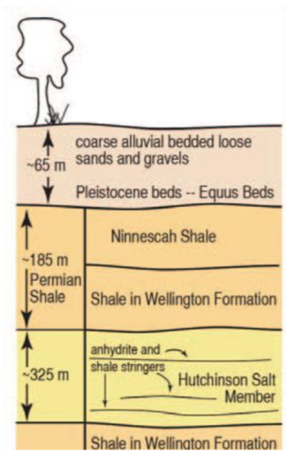

Figure 2. Cartoon representing the generalized geology based on common seismic reflectors of the Hutchinson, Kansas, area (Ivanov, 2013).

Although some individual salt beds may be continuous for only a few miles, the Hutchinson Salt Member as a whole has remarkable lateral continuity. Figure 3 shows the extensive nature of the Permian Hutchinson Salt Member, stretching from central Kansas, northwestern Oklahoma, and into the northeaster portion of the Texas Panhandle. Thickness throughout the Hutchinson Salt is highly variable, averaging around 75 meters and reaching a maximum of over 150 meters towards the south of the basin.

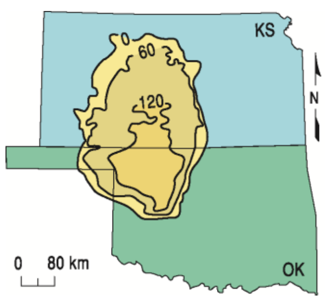

Figure 3. Lateral extent, as well as an isopach of the Hutchinson Salt Member.

Methods

Passive surface wave recording allows random sources of seismic energy (trains, manufacturing facilities, heavy vehicles on roadways, processing plans, heavy construction equipment, etc.), normally considered noise on active surveys, to be used with data processing enhancements and specialized methods to calculate 1D shear wave velocity functions (Louie, 2001; Park et al., 2007, Ivanov et al., 2013). Using this idea, a uniform 2D grid of equal spaced geophones was oriented in close proximity to a nearly perpendicular intersection of two railroad tracks. The trains travelling along the tracks and through this intersection provided ample energy reaching down to approximately 3 Hz in some source files with really good signal.

A previous non-uniform 2D grid proved effective in recording seismic energy with a near-optimal bandwidth and amplitude for interrogating earthen material around the 70 meters deep (Ivanov et al., 2013).

This experiment is part of a larger ongoing investigation with numerous survey lines. However, for this experiment the primary focus are two seismic lines over three known voids: Line 3 and Line 5. To ensure accurate results, a 2D acquisition grid is also analyzed.

2D Grid

A continuous grid of 131 4.5 Hz vertical component geophones spaced 5 meters apart was set up in the shape a square. A square was chosen for symmetry purposes. Shapes such as ellipses favor certain directions over another. The outside was a 70m x 70m square with 3 increasingly smaller squares in the middle. This 2D grid has a record length of 32 seconds and a sample interval of 2 milliseconds. After data acquisition, the grid is pre-processed. In pre-processing, data is converted into the proper format, left-over channels are cut out of the record, and geometry is installed. After the installation of geometry, overtone images are created plotting frequency versus azimuth angle, using commercially available software, SurfSeis 3.0. Using the azimuth, the estimated orientation of the wave front is calculated, to ensure inline planar motion rather than apparent velocities from signal that is oblique to the orientation of the survey lines.

Line 3

Line 3 was oriented east-west and acquired using 126 4.5 Hz vertical component geophones spaced at 3 meters covering a lateral distance of 375 meters and positioned directly over Void #3. The survey used a 32 second record length with a 2 millisecond sample interval. Survey time started approximately 9:00 p.m. and data were acquired

DOI http://dx.doi.org/10.1190/segam2013-1146.1

until 6:30 a.m. of the following day, creating 514 recorded gathers.

The data is converted and cut from rest of the record and geometry is installed. Comparing azimuth angles with low-frequency dominant overtones, a single source is selected for processing. Once a source is selected, that file is then separated into 16 separate records with a spread length of 150 meters and incremented by 15 meters, analogous to an active survey with a moveable array (aka, roll-along).

The extracted records are processed using SurfSeis 3.0 with overtone plots produced with frequency versus phase velocity. Dispersion curves are extracted from these overtone images by picking along the maximum amplitude of the curve (Figure 4). These dispersion curves are then inverted into a 2D Vs profile.

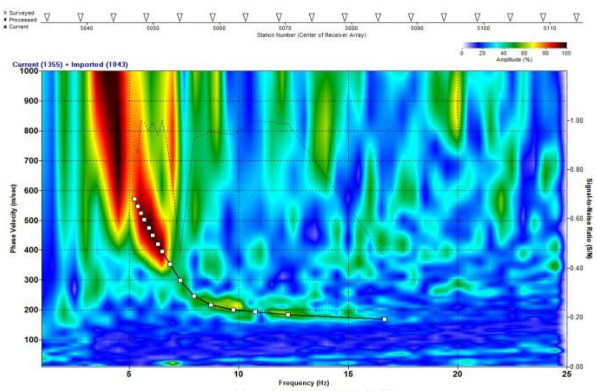

Figure 4. Example of a picked dispersion curve on an overtone.

Line 5

Line 5 was acquired on a separate trip from Line 3, but many of the acquisition parameters are the same. Line 5 consisted of 144 4.5 Hz vertical component geophones oriented parallel to Line 3 and positioned to include Void #1 and Void #2. Line 5 covers approximately 430 meters with geophones spaced every 3 meters. Again a record length of 32 seconds and a 2 millisecond sample interval was used. Survey time started approximately 9:00 p.m. finishing around 7:00 a.m., creating 473 recorded files.

Pre-processing for Line 5 was identical to Line 3, other than the number of extracted records. After choosing a source, 19 records are extracted with a spread length of 150 meters and incremented by 15 meters.

Line 5 is then processed in SurfSeis 3.0 identically to Line 3. The dispersion curves are picked off of the overtone images, and then inverted into a Vs profile.

Results & Discussion

Following processing of Lines 3 and 5, anomalies are identified and characterized. In south central Kansas, drastic changes in shear wave velocity or steeply dipping beds are not common and therefore anomalies of this type should be considered suspect and anomalous.

Line 3

The velocity profile from Line 3 is shown in Figure 5. Notice on this profile the station spacing is 3 meters, creating an imaged lateral distance of approximately 231 meters. The maximum depth of investigation is 90 meters near the void location. The color scale ranges from 150—1200 m/s with higher velocities represented by the hotter colors.

For most of the profile, the lateral change in velocity is almost zero; however there is a very large anomaly towards the western end of the line. The tensional dome of increased shear wave velocity is clearly identified above the location of Void #3. The void is represented by a black star near station number 3080. The tensional dome can extends laterally from approximately stations 3068-3090 a distance of approximately 60 meters. Vertically, the increased velocity can be seen as shallow as 40 meters above the void.

Line 5

Figure 6 shows the velocity profile for Line 5. Again the station spacing is three meters, creating a lateral imaged distance of approximately 270 meters. Maximum depth of investigation is 80 meters. Using the same color scale as Line 3, the hotter colors represent higher velocities and cooler coolers the lower velocities. There are two known voids that are highlighted by the black star near station number 5080 and station number 5095.

Above Void #2 a small tensional dome of increased Vs is observed, however, it is nowhere near the magnitude of Void #3 in Line 3. The top of the dome over Void #2 is observed at approximately 45 meters. Laterally, this feature extends from approximately station numbers 5090-5105, or approximately 45 meters.

Void #1 shows a relatively normal velocity regime, with no tensional dome above the locality of the void. This implies

DOI http://dx.doi.org/10.1190/segam2013-1146.1

there is not a large change in velocity due to the increased stress above the void, as seen above Void #2 and Void #3.

There are a couple potential explanations to the absence of a tensional dome. One potential reason could be the void could be considered immature. Perhaps this void has not migrated upward, therefore not transferring the tensional dome into overlying units. Another possible explanation could be the geometry of the void. The void could be very narrow, not increasing the shear stress above very much at all.

Conclusions

In conclusion, although voids greater than 50 meters in the subsurface are difficult to image using traditional geophysical methods, using passive multichannel analysis of surface waves (MASW) imaging the surrounding rock properties associated with this voids prove a potentially viable technique. The acquisition, processing, and interpretation of passive seismic data successfully imaged an increased shear velocity overlying know subsurface voids.

Passive data were acquired to reach frequencies, and ultimately depths, not possible with active or controlled source surveys. Energy from nearby trains provided the energy sufficient for accurate, comprehensive site characteristics to depths of 90 meters.

The use of the 2D grid is vital to ensure accurate results and correct velocities, by plotting the orientation of the seismic wave propagation in the subsurface. After verifying correct azimuth angle of the wave, linear survey lines are processed to produce 2D Vs vertical plots. Both Line 3 and Line 5 are processed using SurfSeis 3.0 by extracting dispersion curves from the overtone images. These dispersion curves are then compiled and inverted to produce the Vs plots mentioned above.

In both Line 3 and Line 5 a tensional dome is interpreted to be associated with one of the here mentioned voids. These tensional domes are what should be expected above these large subsurface voids due to the lack of rock supporting the weight of overlying units, therefore increasing stress.

Ongoing and future work includes the processing of more lines over other known voids to compare results. Potentially the acquisition of time-lapse data to calculate how the shear wave velocity changes over time.

Acknowledgments

The authors of this paper would like to thank Bevin Bailey, Ryan Nelson and Brett Wedel from the Kansas Geological Survey for help with data acquisition. Also, thanks to Brett Bennett for help with installation of geometry on the front end of the data processing. A special thanks to Tyler Schwenk for help with data acquisition, data processing, and helpful comments.

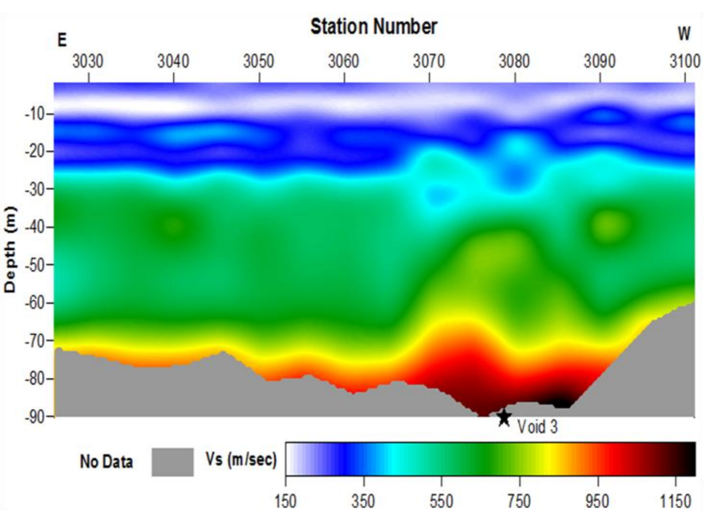

Figure 5. 2D shear wave velocity profile of Line 3. Station spacing of 3 meters.

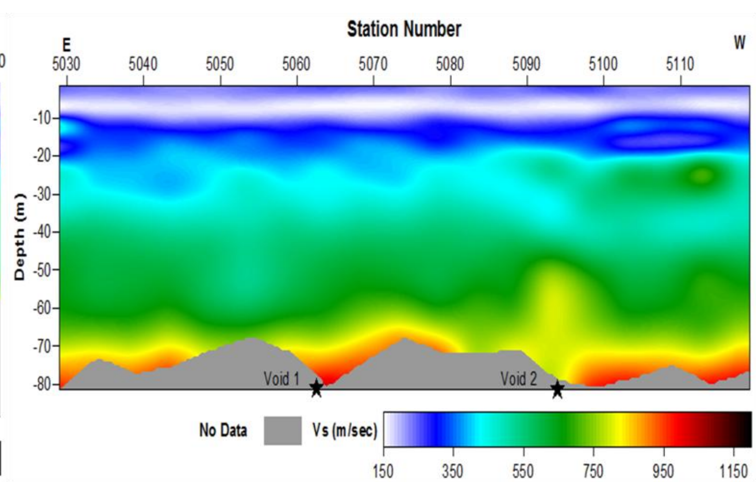

Figure 6. 2D shear wave velocity profile of Line 5. Station spacing of 3 meters.

DOI http://dx.doi.org/10.1190/segam2013-1146.1

http://dx.doi.org/10.1190/segam2013-1146.1

EDITED REFERENCES

Note: This reference list is a copy-edited version of the reference list submitted by the author. Reference lists for the 2013 SEG Technical Program Expanded Abstracts have been copy edited so that references provided with the online metadata for each paper will achieve a high degree of linking to cited sources that appear on the Web.

REFERENCES

Butler, D. K., 1984, Microgravimetric and gravity gradient techniques for detection of subsurface cavities: Geophysics, **49**, 1084–1096, http://dx.doi.org/10.1190/1.1441723.

Davies, W. E., 1951, Mechanics of cavern breakdown: National Speleological Society, **13**, 6–43.

Fenner, T., 1995, Ground-penetrating radar for identification of mine tunnels and abandoned mine stopes: Mining Engineering, **47**, 280–284.

Ivanov, J., B. Leitner, W. Shefchik, J. Shwenk, and S. Peterie, 2013, Evaluating hazards at salt cavern sites using multichannel analysis of surface waves: The Leading Edge, **32**, 298–305, http://dx.doi.org/10.1190/tle32030298.1.

Keiswetter, D., and I. J. Won, 1997, Multifrequency electromagnetic signature of the cloud chamber, Nevada test site: Journal of Environmental & Engineering Geophysics, **2**, no. 2, 99–103, http://dx.doi.org/10.4133/JEEG2.2.99.

Landa, E., V. Shtivelman, and B. Gelchinsky, 1987, A method for detection of diffracted waves on common-offset sections: Geophysical Prospecting, **35**, no. 4, 359–373, http://dx.doi.org/10.1111/j.1365-2478.1987.tb00823.x.

Louie, J. N., 2001, Faster, better: Shear-wave velocity to 100 m depth from refraction microtremor arrays: Bulletin of the Seismological Society of America, **91**, no. 2, 347–364, http://dx.doi.org/10.1785/0120000098.

Miller, R. D., J. Xia, C. B. Park, and J. M. Ivanov, 1999, Multichannel analysis of surface waves to map bedrock: The Leading Edge, **18**, 1392–1396, http://dx.doi.org/10.1190/1.1438226.

Miller, R. D., and D. W. Steeples, 1991, Detecting voids in a 0.6 m coal seam, 7 m deep, using seismic reflection: Geoexploration, **28**, no. 2, 109–119, http://dx.doi.org/10.1016/0016-7142(91)90043-C.

Nolan, J., S. Sloan, S. Broadfoot, J. McKenna, and O. Metheny, 2011, Near-surface void identification using MASW and refraction tomography techniques: 81st Annual International Meeting, SEG, Expanded Abstracts, 1401–1405.

Park, C., and R. Miller, 2008, Roadside passive multichannel analysis of surface waves (MASW): Journal of Environmental & Engineering Geophysics, **13**, no. 1, 1–11, http://dx.doi.org/10.2113/JEEG13.1.1.

Park, C. B., R. D. Miller, and J. Xia, 1999, Multichannel analysis of surface waves: Geophysics, **64**, 800–808, http://dx.doi.org/10.1190/1.1444590.

Park, C., R. Miller, J. Xia, and J. Ivanov, 2007, Multichannel analysis of surface waves (MASW) — Active and passive methods: The Leading Edge, **26**, 60–64, http://dx.doi.org/10.1190/1.2431832.

Peterie, S. L., R. D. Miller, and D. W. Steeples, 2009, Diffraction imaging versus reflection processing for shallow void detection: 78th Annual International Meeting, SEG, Expanded Abstracts, **28**, 1421–1424.

Sloan, S. D., S. L. Peterie, J. Ivanov, R. D. Miller, and J. R. McKenna, 2010, Void detection using near-surface seismic methods: Advances in near-surface seismology and ground-penetrating radar: SEG Geophysical Developments Series, **15**, 201–218.

Turpening, R. M., 1976, Cavity detection by means of seismic shear and compressional wave refraction techniques: Report 116400-1-F, Environmental Research Institute of Michigan.

Walters, S. L., R. D. Miller, D. W. Steeples, J. Xia, and C. Zeng, 2009, Detecting tunnels and underground facilities using diffracted P-waves: Proceedings of the 22nd Annual Symposium on the Application of Geophysics to Environmental and Engineering Problems, **22**, 937–942.

DOI http://dx.doi.org/10.1190/segam2013-1146.1